

## Frequency dependent specific heat of viscous silica

Peter Scheidler, Walter Kob \*, Arnulf Latz, Jürgen Horbach, and Kurt Binder  
*Institut für Physik, Johannes Gutenberg-Universität, Staudinger Weg 7, D-55099 Mainz,  
 Germany*

### Abstract

We apply the Mori-Zwanzig projection operator formalism to obtain an expression for the frequency dependent specific heat  $c(z)$  of a liquid. By using an exact transformation formula due to Lebowitz *et al.*, we derive a relation between  $c(z)$  and  $K(t)$ , the autocorrelation function of temperature fluctuations in the microcanonical ensemble. This connection thus allows to determine  $c(z)$  from computer simulations in equilibrium, i.e. without an external perturbation. By considering the generalization of  $K(t)$  to finite wave-vectors, we derive an expression to determine the thermal conductivity  $\lambda$  from such simulations. We present the results of extensive computer simulations in which we use the derived relations to determine  $c(z)$  over eight decades in frequency, as well as  $\lambda$ . The system investigated is a simple but realistic model for amorphous silica. We find that at high frequencies the real part of  $c(z)$  has the value of an ideal gas.  $c'(\omega)$  increases quickly at those frequencies which correspond to the vibrational excitations of the system. At low temperatures  $c'(\omega)$  shows a second step. The frequency at which this step is observed is comparable to the one at which the  $\alpha$ -relaxation peak is observed in the intermediate scattering function. Also the temperature dependence of the location of this second step is the same as the one of the  $\alpha$ -peak, thus showing that these quantities are intimately connected to each other. From  $c'(\omega)$  we estimate the temperature dependence of the vibrational and configurational part of the specific heat. We find that the static value of  $c(z)$  as well as  $\lambda$  are in good agreement with experimental data.

PACS numbers: 61.20.Lc, 61.20.Ja, 02.70.Ns, 64.70.Pf

Typeset using REVTeX

---

\*Author to whom correspondence should be addressed to. e-mail: Walter.Kob@uni-mainz.de

## I. INTRODUCTION

If a glass-forming liquid is cooled, dynamic observables, such as the viscosity, the diffusion constant or the intermediate scattering function, show a dramatic slowing down [1,2]. At a certain temperature, the kinetic glass transition temperature  $T_g$ , the typical relaxation time of the system exceeds the time scale of the experiment and the system falls out of equilibrium, i.e. become a glass [3]. In contrast to these *dynamical* observables, all *static* quantities, such as the volume or the enthalpy, show upon cooling only a relatively weak temperature dependence for  $T > T_g$  and the glass transition temperature is noticed only by a gentle change of slope in their temperature dependence. This change of slope is reflected in various susceptibilities, such as the thermal expansion coefficient or the specific heat  $c_V$ , as a relatively sudden drop when the glass transition temperature is reached. The physical picture behind this drop in, e.g.,  $c_V$  is that at  $T_g$  the structural degrees of freedom fall out of equilibrium and the specific heat reduces to the one of a solid having only vibrational degrees of freedom. Hence the height of the drop is usually used to estimate that part of the specific heat associated with the configurational degrees of freedom. Thus we see that this type of experiments can be used to probe the dynamics of the structural degrees of freedom, although the information obtained is rather indirect.

Since the value of  $T_g$  is given by the timescale of the experiment, it can be changed if the sample is cooled with different cooling rates [4,5]. Therefore this dependence opens in principle the possibility to investigate the temperature dependence of the configurational part of the specific heat. However, since the relaxation time of the system changes very rapidly with temperature, it is necessary to change the cooling rate significantly (several decades) in order to see a significant shift in  $T_g$ , which is experimentally rather difficult. An alternative way to probe the dynamics of the structural degrees of freedom by means of the specific heat is to measure  $c(z)$ , the (complex) frequency dependence of the specific heat of the system *in its equilibrium state*. Seminal work in this direction was done by Nagel and coworkers [6–10] who proposed an experimental setup that allowed to measure  $c(z)$  also at frequencies as high as  $10^4$  Hz. Independent work in this direction was also done by Christensen and others [11–14].

Using their measurements of the frequency dependence of the specific heat, Jeong and Moon were able to predict cooling and heating curves in differential scanning calorimetry (DSC) and found good agreement between their predicted curves and the experimental ones [13]. Similar results have been found in molecular dynamics computer simulations [15,16]. Thus these investigations give evidence that the information contained in the equilibrium quantity  $c(z)$  allows one to understand also the out-of-equilibrium situation that is encountered in DSC experiments around  $T_g$ . A short review of this can be found in the paper by Simon and McKenna [17].

The theoretical interpretation of the measurements of  $c(z)$  was for some time rather controversial [18–23] since the origin of the frequency dependence of  $c(z)$  was not really clear. Some of these issues could be clarified by experiments done by Birge [7] and Menon [10]. A partial discussion of this dispute is reviewed in Ref. [17]. Very recently Nielsen put forward a theoretical description of  $c(z)$  on purely thermodynamic arguments [24]. In the present paper we will use a statistical mechanics approach to derive a microscopic expression for  $c(z)$  and use this expression, which is identical to the one derived independently in

Ref. [24], to calculate this quantity from a molecular dynamics computer simulation of silica. Interestingly enough this expression has been used before by Grest and Nagel [25] to calculate  $c(z)$  from a computer simulation of a simple liquid. However, in that paper no derivation was given since it seems to have come out “from a stroke of genius” [26]. Due to limitations of computer resources the resulting curves for  $c(z)$  were unfortunately rather noisy, a feature they share with the ones in Ref. [24]. In contrast to this, great care was taken in the present work to obtain reliable data, which in turn allows us to compare the temperature dependence of  $c(z)$  with the one from other dynamical quantities, such as the intermediate scattering function. Thus this permits us to compare the relaxation dynamics as probed by  $c(z)$  with the one observed by more microscopic methods, such as neutron or light scattering experiments.

The outline of the paper is as follows: In the next section we will use the projection operator formalism to derive a connection between  $c(z)$  and microscopic variables. In Sec. III we will give the details of the model and the simulations. In Sec. IV we will present the results and end in Sec. V with a summary and discussion.

## II. THEORY

In this section we derive an expression that relates the frequency dependent specific heat to the autocorrelation function of kinetic energy fluctuations. Furthermore we show how the thermal conductivity can be calculated from the generalization of this correlation function to finite wave-vectors.

For a dense simple liquid under triple point conditions the only slow modes are the local densities of the macroscopically conserved quantities, i.e. the number of particles, the total momentum, and the energy. For an  $N$ -particle system these local densities have the form

$$X(\mathbf{r}, t) = \sum_{i=1}^N X_i(t) \delta(\mathbf{r} - \mathbf{r}_i(t)), \quad (1)$$

where for  $X_i(t) = 1$  we obtain the local density fluctuation  $\rho(\mathbf{r}, t)$ , for  $X_i(t) = p_i^\alpha$  the momentum density in direction  $\alpha \in \{x, y, z\}$ , and for  $X_i(t) = E_i := \mathbf{p}_i^2/2m + \frac{1}{2} \sum_{j=1}^N V(|\mathbf{r}_i - \mathbf{r}_j|)$  the local energy density fluctuation. (Here  $V(\mathbf{r})$  is the potential energy.) In the hydrodynamic limit the equation of motion for these densities can be derived by using the exact conservation laws, some (phenomenological) constitutive equations that relate the spatial derivatives of the densities to their currents, and thermodynamic relations between the fluctuations of the densities and thermodynamic quantities such as temperature, pressure etc. [27]. This approach is valid as long as there are no other slow, non-hydrodynamic processes in the system. Well known examples, for which constitutive equations and thermodynamic relations have to be modified by, e.g., introducing frequency dependent thermodynamic derivatives, are second order phase transitions or systems with internal degrees of freedom [28].

As mentioned in the Introduction, the dramatic slowing down of the dynamics of liquids upon cooling is observed on all length scales. But contrary to second order phase transitions no long range order is building up in two particle correlation functions, since the slowing down of the dynamics seems not to be caused by a growing correlation length. Instead the physical origin for the slow dynamics is the local hindering of the particle motion, the so-called cage-effect, i.e. it is due to a mechanism operating on the *microscopic* scale. However,

the consequences of this local slowing down can of course also be detected on mesoscopic and macroscopic length scales, e.g. in thermodynamic derivatives, as soon as the time scale of the experiment is comparable to the time scale of the structural relaxation.

In Ref. [21] a formally exact method to derive frequency dependent constitutive equations and thermodynamic derivatives in the canonical ensemble was introduced, which thus allows to investigate the consequences of the slowing down of the structural relaxation on thermodynamic and hydrodynamic quantities. The main technical tools in that paper are thermodynamic response theory and projection operator techniques. In such an approach the most important physical ingredient is the appropriate microscopic definition of the temperature  $\theta(\mathbf{r}_i, \mathbf{p}_i)$  as a function of the phase space variables  $\mathbf{r}_i$  and  $\mathbf{p}_i$ . From a *mathematical* point of view the choice of a such a function is not unique since the only condition one has to fulfill is that

$$\langle \theta(\mathbf{r}_i, \mathbf{p}_i) \rangle = T \quad , \quad (2)$$

where  $T$  is the macroscopic temperature. For the case of supercooled liquids also *physical* considerations impose restrictions to the possible set of functions: In the canonical ensemble the temperature of the system is imposed by an external heat bath. Therefore the definition of the phase space function  $\theta(\mathbf{r}_i, \mathbf{p}_i)$  should allow that Eq. (2) holds also in the case that  $T$  is changing on a time scale that is shorter than the one of the structural relaxation. (Such rapid changes occur, e.g., in the earlier mentioned experiments on the frequency dependent specific heat. But also for the case of a glass below  $T_g$  the concept of a temperature is useful, despite the fact that the true relaxation time of the system is exceedingly large.) Since structural relaxation is related to rearrangements in space, it can be expected that definitions of  $\theta(\mathbf{r}_i, \mathbf{p}_i)$  that involve the positions  $\mathbf{r}_i$  do not fulfill the requirement of being “fast”. Momentum, instead, can quickly be exchanged between particles, and hence is transferred easily through the system. An appropriate microscopic definition of a temperature, obeying the mentioned mathematical and physical requirements, can be constructed with the help of the kinetic energy of a particle,

$$\theta(\mathbf{r}_i, \mathbf{p}_i) \equiv \theta(\mathbf{p}_i) = \frac{1}{3k_B m} \mathbf{p}_i^2 \quad . \quad (3)$$

The canonical average  $\langle \theta(\mathbf{p}_i) \rangle$  is, as required, the macroscopic temperature  $T$ . However, if one wants to define a *local* density related to the temperature, it can of course not be avoided that there is a dependence on spatial variables. Thus the best one can do is to make this dependence as simple as possible so that it is possible to extract the fast part easily. For a classical system a convenient microscopic definition of a local temperature field is therefore

$$T(\mathbf{r}, t) = \sum_i \theta(\mathbf{p}_i) \delta(\mathbf{r} - \mathbf{r}_i(t)) \quad . \quad (4)$$

The canonical average  $\langle T(\mathbf{r}, t) \rangle$  is given by  $nT$ , where  $n = N/V$  is the number density. Although it is not a conserved quantity, in supercooled liquids the temperature field  $T(\mathbf{r}, t)$  has a slow component, due to its dependence on the positional degrees of freedom. However, the fast fluctuation part can easily be obtained by projecting out these slow density fluctuations:

$$\delta T(\mathbf{r}, t) = T(\mathbf{r}, t) - T\rho(\mathbf{r}, t) \quad (5)$$

or in Fourier space

$$\delta T_q(t) = T_q(t) - T\rho_q(t) \quad . \quad (6)$$

Note that by construction this temperature fluctuation does not have any static coupling to functions of the form  $G_q(\mathbf{r}^N) = G(\mathbf{r}^N) \exp(i\mathbf{q} \cdot \mathbf{r}_i)$ , i.e. that depend only on the positions of the particles:

$$\langle \delta T_q^* G_q(\mathbf{r}^N) \rangle = 0 \quad , \quad (7)$$

which shows that its dynamic autocorrelation function  $\Phi_{TT}(q, t) = (T_q(t)|T_q)$  cannot be proportional to any multi-point density correlation function. (For later use we have introduced the notation  $(A|B) := \langle \delta A^* \delta B \rangle$ .) Although it is not possible to prove from the Ansatz (5) that  $\delta T_q(t)$  is really a fast variable for  $q > 0$ , i.e. that it does not undergo a structural arrest in the canonical ensemble, this is something that can be checked in simulations and below we will demonstrate that this is indeed the case. Note, however, that the *time* dependence of the temperature fluctuations is of course affected by the slowing down of structural relaxation. This was derived in [21] within linear response theory. In the following we will briefly sketch the main steps in that derivation in order to clarify the physics behind the final results.

Since in this paper we are interested in the frequency dependent specific heat per particle at constant volume, the first thing to do is to derive a microscopic expression for this quantity and to relate it to the local fluctuations of the temperature. For the sake of simplicity we will focus on the case of temperature fluctuations for vanishingly small wave-vectors, since in this limit they decouple from the single particle density and current fluctuations. (However, in the last part of this section we will also consider finite wave-vectors.) To determine  $c_v(z)$  we have to calculate, in analogy to the *static* case  $\Delta E = c_v^{eq} \Delta T$ , the effect of temperature fluctuations on fluctuations of the total energy. For this let us assume that we impose adiabatically at time  $t = 0$  a (small) temperature fluctuation  $\delta T_q^*(t)$ . In this case the initial probability distribution in the canonical ensemble is

$$\frac{\exp(-\beta(H - h\delta T_q))}{\text{Tr} \exp(-\beta(H - h\delta T_q))} \quad , \quad (8)$$

where  $h$  is the conjugate field of  $\delta T_q$  and  $\beta = 1/k_B T$ .

In the linear response regime the time evolution of any variable  $Y^*(t)$  is given by

$$\langle Y^*(t) \rangle_{NE} = \langle Y^*(t) \rangle + h \beta (Y(t)|T_q) \quad , \quad (9)$$

where the average on the lefthand side is done in the non-equilibrium ensemble (8), and the one on the righthand side are performed in the standard canonical ensemble ( $h = 0$  in Eq. (8)). Using Eq. (9) for the case  $Y = T_q$  we thus obtain for the time dependence of the temperature fluctuation

$$\langle \delta T_q^*(t) \rangle = h \beta (T_q(t)|T_q) = h \beta \Phi_{TT}(t) \quad , \quad (10)$$

and the relaxation of a fluctuation of the energy, Eq. (1) with  $X_i = E_i$ , is given by

$$\langle \delta E_q^*(t) \rangle = h \beta (E_q(t)|T_q) \quad . \quad (11)$$

In analogy to the static case we define the frequency dependent specific heat  $c_v(z)$  as the coefficient between the fluctuation in the energy and the one in temperature:

$$\langle \delta E_q^*(z) \rangle = c_v(z) \langle \delta T_q^*(z) \rangle \quad , \quad (12)$$

where  $\delta E_q(z)$  and  $\delta T_q(z)$  are the Laplace transforms of  $\delta E_q(t)$  and  $\delta T_q(t)$ , respectively. Hence we now have to express  $(E_q(t)|T_q)$  from Eq. (11) as a functional of  $\delta T_q(t)$ . The Laplace transform of  $(E_q(t)|T_q)$  is  $(E_q|R(z)|T_q)$ , with the resolvent  $R(z) = 1/(\mathcal{L} - z)$  and the Liouville operator  $\mathcal{L}$ . Using a projection operator formalism with the operator  $P = |\delta T_q\rangle\langle \delta T_q|(\delta T_q|\delta T_q)^{-1}(\delta T_q|$  to project on temperature fluctuations, the correlator  $(E_q|R(z)|T_q)$  can be written as [21]

$$(E_q|R(z)|T_q) = \{(E_q|T_q) - (E_q|R'(z)|\mathcal{L}T_q)\} \frac{1}{S_{TT}^c} \langle \delta T_q^*(z) \rangle \quad . \quad (13)$$

Here  $R'(z) := Q/(Q\mathcal{L}Q - z)$ , with  $Q = 1 - P$ , is the reduced resolvent which describes the dynamics in the directions of phase space perpendicular to temperature fluctuations (and by using the more general formalism from Ref. [21] also perpendicular to density and current fluctuations). The quantity  $S_{TT}^c$  is defined as

$$S_{TT}^c = \langle \delta T_q^*(0)\delta T_q(0) \rangle = 2NT^2/3 \quad , \quad (14)$$

and is independent of  $q$ . (The superscript  $c$  indicates the canonical ensemble.) From Eq. (13) the expression for the specific heat can be read off. We introduce the projection operators  $P_\rho := |\rho_q\rangle\langle \rho_q|(\rho_q|\rho_q)$  and  $Q_\rho := 1 - P_\rho$  and use the equations

$$\mathcal{L}Q_\rho E_q^K = -\mathcal{L}Q_\rho E_q^P + \mathcal{O}(q) = -\mathcal{L}Q E_q^P \quad (15)$$

$$\frac{-Q\mathcal{L}Q}{z - Q\mathcal{L}Q} = Q - \frac{zQ}{z - Q\mathcal{L}Q} \quad , \quad (16)$$

where  $E_q^K$  and  $E_q^P$  are the Fourier transform of the kinetic and potential energy fields  $E^K(\mathbf{r})$  and  $E^P(\mathbf{r})$ , respectively [29]. The specific heat can now be expressed as

$$c_v(z) = c_v^{eq} + \frac{\beta}{NT} \lim_{q \rightarrow 0} z (E_q^P|R'(z)|E_q^P) \quad , \quad (17)$$

where  $c_v^{eq} = c_v = \frac{\beta}{NT} \lim_{q \rightarrow 0} (E_q|Q_\rho|E_q)$  is the equilibrium value of the specific heat [30] per particle. We emphasize, that Eq. (17) is an exact expression for the frequency dependent specific heat at constant volume. It only relies on Eq. (5) as a physical reasonable definition of temperature fluctuations.

Expression (17) reveals the physical origin of the frequency dependence of the specific heat very clearly: During the process of structural relaxation the system probes the potential energy landscape. This dynamics is governed by the (slow) relaxation of the densities and their higher order products and hence gives rise to a nontrivial slow dynamics even in the projected dynamics  $R'(z)$ , although the latter does not contain any hydrodynamic poles.

Expression (17) is the ideal starting point for approximation schemes like the mode coupling theory. However, for exact calculations of  $c_v(z)$ , e.g. in computer simulations, it cannot be used, since it is not possible to implement the projected dynamics. To solve this problem we will now express  $c_v(z)$  in terms of correlation functions that can be measured in a real dynamics, such as  $\Phi_{TT}(q, t)$ . For this we make use of Refs. [21,31] where similar calculation as just presented for  $c_v(z)$  were done for  $c_p(z)$ , the specific heat at constant pressure, as well as the frequency dependent heat conduction coefficient  $\tilde{\lambda}(z)$ . Using these results it can be shown that for small wave-vectors the Laplace transform of  $\Phi_{TT}(q, t)$  obeys the exact equation of motion

$$\begin{aligned} \Phi_{TT}(q, z) &:= i \int_0^t dt \exp(izt) \langle \delta T_q^*(t) \delta T_q(0) \rangle \\ &= \frac{-S_{TT}^c 3k_B/2}{z c_p(z) + \tilde{\lambda}(z) q^2 - z^3 \frac{c_p(z) - c_v(z)}{z^2 - q^2 K_B(z)/mn}} \quad , \end{aligned} \quad (18)$$

where  $K_B(z)$  is the frequency dependent bulk modulus and  $n$  is the particle density [21,31]. Although in general  $\tilde{\lambda}$  depends on frequency  $z$ , theoretical arguments show [21] that in supercooled liquids this dependence is only weak, in agreement with experimental findings [7]. Therefore  $\tilde{\lambda}(z)$  can be replaced by its static value,  $\tilde{\lambda}(z=0) = i\lambda/n$ , where  $\lambda$  is the equilibrium heat conduction coefficient [32]. Note that the form for the equation for  $\Phi_{TT}(q, z)$  is exactly as the one in linearized hydrodynamics [27] except that now the transport coefficients *and* the thermodynamic derivatives are generalized to functions of the complex frequency  $z$ .

In the limit of vanishing wave-vectors we thus obtain from Eq. (18) the following relation between  $\Phi_{TT}(q, z)$  and  $c_v(z)$ :

$$\lim_{q \rightarrow 0} \frac{\Phi_{TT}(q, z)}{S_{TT}^c} = \frac{-3k_B}{2z c_v(z)} \quad . \quad (19)$$

We emphasize that  $c_v(z)$  as it occurs in Eqs. (18) and (19) is exactly the dynamic specific heat from Eq. (12) that relates fluctuations in temperatures to the ones in energy. Using Eq. (19), we thus can express this dynamic specific heat by a standard correlation function:

$$c_v(z) = \frac{-3k_B S_{TT}^c}{2z \Phi_{TT}(q=0, z)} \quad . \quad (20)$$

Therefore we find that in the canonical ensemble the specific heat can be expressed by the autocorrelation function of the temperature fluctuations, a quantity which is readily accessible in simulations. (An equivalent definition of the specific heat in terms of potential energy fluctuations is given in [33]).

It is important to note that the expression (18) for  $\Phi_{TT}$  is valid only in the *canonical* ensemble. To obtain the corresponding relation in the *microcanonical* ensemble, a general transformation due to Lebowitz *et al.* can be used [34], which relates averages of time dependent functions in the canonical ensemble to their averages in the microcanonical ensemble. Denoting  $\delta T(q=0)$  by  $\delta T_0$  we thus obtain:

$$\Phi_{TT}(t) = \langle \delta T_0^*(t) \delta T_0 \rangle_c = \langle \delta T_0^*(t) \delta T_0 \rangle_{mc} + \frac{\beta^2 k_B}{N c_v^{eq}} \left| \frac{\partial \langle T_0 \rangle}{\partial \beta} \right|^2$$

$$\begin{aligned}
&= \Phi_{TT}^{(mc)}(t) + \frac{N\beta^2}{k_B c_v^{eq}} \left( \frac{\partial 1/\beta}{\partial \beta} \right)^2 \\
&= \Phi_{TT}^{(mc)}(t) + \frac{N}{c_v^{eq} k_B \beta^2} \quad .
\end{aligned} \tag{21}$$

Here we used, that  $\langle T_0 \rangle = NT$  [35]. If we set  $t = 0$ , the equilibrium specific heat  $c_v^{eq}$  can thus be written as

$$\frac{3k_B}{2c_v^{eq}} = 1 - K(0) \quad , \tag{22}$$

where we have introduced the normalized temperature autocorrelation function

$$K(t) := \Phi_{TT}^{(mc)}(t)/S_{TT}^c \quad . \tag{23}$$

Putting this back into Eq. (21) and using Eq. (20) we finally obtain

$$c_v(z) = \frac{3k_B/2}{1 - K(t=0) - zLT[K(t)](z)} \quad , \tag{24}$$

where  $LT$  stands for the Laplace transform.

Equation (24), with a slightly different definition of the function  $K(t)$ , was first used in [25] as an ad hoc generalization of Eq. (22) to non-vanishing frequencies and later derived within thermodynamic response theory by Nielsen [24].

So far we have focused on the autocorrelation function of  $T_q$  in the limit  $q \rightarrow 0$ . In the following we will now consider the case  $q > 0$ . From Eq. (18) it follows immediately that for small but not vanishing  $q$  the decay of  $\Phi_{TT}(q, t)$  is dominated by the hydrodynamic pole at  $\omega = -iD_T q^2$  with  $D_T = \lambda/(nc_p^{eq})$ . Below we will see that it is important to consider also corrections of order  $q^2$  to  $D_T$ . As it will turn out, the frequency dependence of the specific heat will give the main contribution in these corrections. From theoretical considerations [21] as well as from experiments [7] we know that the heat conduction coefficients do not (or only very weakly) depend on frequency. In analogy to the specific heat at constant volume,  $c_v(z)$ , the specific heat at constant pressure,  $c_p(z)$ , will also depend on frequency. Using a generalization of Legendre transformations between different thermodynamic ensembles it can be shown that  $c_p(z)$  can be written in the form  $c_p(z) = c_p^{eq} + z\Delta(z)$ , where  $\Delta(z)$  is a frequency dependent function with a positive spectrum [31]. For  $z = \omega + i\epsilon$ , it is given by  $\lim_{\epsilon \rightarrow 0} \Delta(\omega + i\epsilon) = \Delta'(\omega) + i\Delta''(\omega)$ . The value of  $\Delta''(\omega)$  at  $\omega = 0$  has several contributions, one being proportional to the longitudinal viscosity  $\eta_l = \eta_V + \frac{4}{3}\eta_S$ , where  $\eta_V$  and  $\eta_S$  are the bulk and shear viscosity, respectively. The relaxation time  $\tau_q$  of  $\Phi_{TT}(q, t)$  which is related to the hydrodynamic pole can be calculated by determining the frequency at which the main denominator of Eq. (18) vanishes up to order  $q^6$ . Making the Ansatz  $1/\tau_q = \omega_R = -iD_T q^2 + iBq^4 - Aq^4$  we obtain

$$\omega_R = -iD_T q^2 \left( 1 - \frac{\Delta''(\omega=0)}{c_p^{eq}} D_T q^2 + \frac{\gamma-1}{K_B \gamma / mn} D_T^2 q^2 \right) + D_T^2 \frac{\Delta'(\omega=0)}{c_p^{eq}} q^4 \quad , \tag{25}$$

where  $\gamma$  is  $c_p^{eq}/c_v^{eq}$ ,  $\gamma - 1$  is the Landau - Placzek ratio, and  $K_B$  is the static bulk modulus. The real part indicates an experimentally undetectable shift of the position of the Rayleigh



peak to finite frequencies. Since it is the frequency of an overdamped harmonic oscillation, it does not influence the relaxation time  $\tau_q$  of the correlator in real time. From Eq. (25) the relaxation time up to order  $q^0$  of the exponentially decaying temperature autocorrelation function is thus given by

$$\tau_q = \frac{1}{\omega_R} = \frac{nc_p^{eq}}{\lambda} \frac{1}{q^2} + \frac{\Delta''(\omega=0)}{c_p^{eq}} - D_T \frac{\gamma-1}{K_B \gamma / mn} + \mathcal{O}(q^2) . \quad (26)$$

It is interesting to note that for the case of supercooled liquids the term proportional to  $q^0$  is only positive due to the existence of a frequency dependent specific heat, i.e. that  $\Delta'' > 0$ . Without it, the subtraction of the positive Landau-Placzek ratio  $\gamma - 1$  would lead to a negative offset in a plot of  $\tau_q$  against  $1/q^2$ . Below we will check the validity of this  $q$ -dependence and calculate from this relation the value of  $\lambda$ . Note that in the case of *finite* wave-vectors the autocorrelation functions  $\langle \delta T_q^*(t) \delta T_q(0) \rangle$  in the canonical and microcanonical ensemble are identical, and hence it is not necessary to use the transformation formula of Lebowitz *et al* [34].

### III. MODEL AND DETAILS OF THE SIMULATIONS

In this section we discuss the system we used to test the ideas presented in the previous section and give the details of the simulations. At the end we also briefly discuss the influence of finite size effects on the results.

Although the formalism presented in the previous section is of course applicable to all types of glass forming liquids, it is of special interest to investigate a system which exists also in reality, since this opens the possibility to compare the results from the simulations with those from experiments. To do a simulation of a real material one needs a potential that describes reliably the interactions between the atoms of this substance. In the case of silica such a potential does indeed exist, since a decade ago van Beest *et al.* (BKS) used *ab initio* calculations to obtain a classical force field for this material [36]. The functional form of this potential is given by

$$\phi_{\alpha\beta}(r) = \frac{q_\alpha q_\beta e^2}{r} + A_{\alpha\beta} \exp(-B_{\alpha\beta} r) - \frac{C_{\alpha\beta}}{r^6} \quad \alpha, \beta \in [\text{Si}, \text{O}], \quad (27)$$

where  $r$  is the distance between two ions of type  $\alpha$  and  $\beta$ . The value of the constants  $q_\alpha, q_\beta, A_{\alpha\beta}, B_{\alpha\beta}$ , and  $C_{\alpha\beta}$  can be found in Ref. [36]. The short range part of the potential was truncated and shifted at a distance of 5.5Å, which leads to a better agreement of the results for the density of vitreous silica as predicted from this model with the experimental values [5]. In the past it has been shown that this potential is able to reproduce reliably various properties of amorphous silica, such as its structure, its vibrational and relaxational dynamics, the static specific heat below the glass transition temperature, and the conduction of heat [5,37–47]. Thus it is reasonable to assume that this potential will also reproduce well the quantities needed to calculate the frequency dependent specific heat, i.e. the correlation function  $K(t)$  in Eq. (23).

Using the BKS potential, the equations of motion were integrated with the velocity form of the Verlet algorithm with a time step of 1.6fs. The sample was first equilibrated by coupling it every 50 time steps to a stochastic heat bath for a time which allowed the system

to relax at the temperature of interest. (We assumed a sample to be relaxed if the coherent intermediate scattering function at the wave-vector corresponding to the main peak in the static structure factor had decayed to zero within the time span of the equilibration [48].) After this equilibration we started a microcanonical run for the production from which we determined the equilibrium dynamics at various temperatures. The temperatures investigated were 6100K, 4700K, 4000K, 3580K, 3250K, 3000K, and 2750K. At the lowest temperature  $K(t)$  decays so slowly that runs with 30 million time steps were needed to equilibrate the sample, which corresponds to a real time of 49ns. All the simulations were done at a constant density of 2.36g/cm<sup>3</sup> which corresponds to a pressure around 0.87 GPa [15]. Since the temperature expansion coefficient of silica is small [5,49], it can be expected that a constant pressure simulation would basically give the same results as our simulation.

To obtain also results in the glass at room temperature we cooled the sample from 3000K to 2750K with a cooling rate around  $3 \cdot 10^{11}$ K/s, and then rapidly quenched it to 300K. The so obtained glass was annealed for additional 300,000 time steps before we started the measurement of the various quantities.

Since the main observable of interest,  $K(t)$ , is a collective variable, it has a relatively large statistical error. Therefore we averaged all the runs over 200 independent samples for  $T \geq 4700$ K, over 100 samples for  $4000\text{K} \geq T \geq 3000\text{K}$ , and 50 samples for  $T = 2750\text{K}$ . In order to make so many independent runs the system size had to be rather small. Therefore we choose a system of 112 silicon and 224 oxygen ions in a cubic box of size 18.8Å. The Coulombic part of the potential was evaluated with the Ewald method and a parameter  $\alpha$  of  $7.5\text{Å}^{-1}$ . All these calculations took around 8 years of single CPU time on a parallel computer with high end workstation processors.

As it was shown in Refs. [47,50], the *dynamics* of network glass formers shows quite strong finite size effects since the small systems lack the acoustic modes at small wave-length. Thus it can be expected that if we determine  $K(t)$  for a system of 336 particles the result will be different from the ones for a system of macroscopic size. In order to check the influence of the system size on our results we have made some test runs with 1008 particles and found, in agreement with the results of Refs. [47,50], that at long times the dynamics of the larger system is a bit faster than the one of the small one [15]. However, the qualitative behavior of the various relaxation functions are independent of the system size and therefore we can expect that the results presented in this work will hold also for larger systems.

#### IV. RESULTS

In this section we present the results from our simulation, i.e. the temperature dependence of  $K(t)$  and the frequency dependence of the specific heat. At the end we briefly discuss the time and temperature dependence of the generalization of  $K(t)$  to finite wave-vectors.

As it is obvious from Eq. (24), the first step in the calculation of the frequency dependent specific heat is to determine  $K(t)$ , the autocorrelation function of the fluctuation in the kinetic temperature. Since  $K(t)$  is a collective quantity it is relatively difficult of determine it with high accuracy. This is shown in Fig. 1a where we plot  $K(t)/K(0)$  at  $T = 3000\text{K}$ . Each of the thin curves corresponds to the average over ten independent samples. From the figure we recognize that even if the shape of the different curves is quite similar, their height

varies considerably. Thus one should realize that even if the average over 100 samples gives a quite nice and smooth curve (bold solid curve) it still might be subject to a significant statistical error.

In Fig. 1b we show the time dependence of  $K(t)/K(0)$  for all temperatures investigated. From this figure we see that for all temperatures this correlator decays within  $10^{-2}$ ps to a value smaller than 0.2, i.e. very rapidly. For the highest temperatures  $K(t)$  then shows a small shoulder at around 0.01ps, a feature which, at these temperatures, is not observed in correlation functions such as the intermediate scattering function  $F(q, t)$ , where  $q$  is the wave-vector [42,45]. (See Ref. [48] for a definition of  $F(q, t)$ ). With decreasing temperature this shoulder extends to larger and larger times until we observe at the lowest temperature a well defined plateau which extends over several decades in time. Thus from this point of view  $K(t)$  behaves qualitatively similar to  $F(q, t)$ . Since for this quantity it is customary to refer to this final decay as the “ $\alpha$ -relaxation” we will use the same term in the case of  $K(t)$  as well. Note that the height of the plateau in  $K(t)$  is only around 0.1, which shows that most of the correlation of the kinetic energy is lost during the brief ballistic flight of the particles,  $t \leq 10^{-2}$ ps, inside the cage.

From the figure we also see that with decreasing temperature the correlation function starts to show a minimum at short times. The reason for this feature is that at low temperatures and short times the system behaves similar to a harmonic solid and thus it can be expected that the connection between  $K(t)$  and the velocity-autocorrelation function  $J(t)$ , see Eq. (A7) in the Appendix, starts to hold. (We remind the reader that in supercooled liquids the velocity-autocorrelation function shows a dip at short times.) That this is indeed the case is demonstrated in Fig. 1c, where we compare the two correlators at a high and a low temperature. We see that for  $T = 300$ K, i.e. in the glass where the harmonic approximation is valid,  $K(t)$  and  $J(2t)$  are identical within the accuracy of the data (solid lines). For temperatures at which the system is still able to relax the situation is different. At short times  $K(t)$  (bold dashed line) shows oscillations with extrema which are located at the same times at which also  $J(2t)$  (thin dashed line) shows maxima and minima. Thus the harmonic-like character of the motion on these time scales is clearly seen. For larger times, however,  $J(2t)$  goes rapidly to zero whereas  $K(t)$  shows the above discussed plateau before it decays to zero at very long times.

In order to investigate this point in more detail we can make use of Eq. (A8), which relates the spectrum of  $K(t)$ ,  $\hat{K}(\omega)$ , to  $g(\omega)$ , the time Fourier transform of the velocity-autocorrelation function. At low temperatures the latter quantity is nothing else than the density of states of the system. (In order to calculate these Fourier transforms we made use of the Wiener-Khinchin theorem which relates the power spectrum of a time dependent signal to the Fourier transform of the corresponding autocorrelation function [51].) In Fig. 2 we show  $\hat{K}(\omega)$  for a temperature in the melt and in the glass (dashed lines) and compare these curves with  $g(\omega/2)/8$  at the same temperatures (solid lines). We see that, within the accuracy of our data, in the glass the two curves are indeed identical. (We remind the reader that the two peaks at high frequencies correspond to intra-tetrahedral motion of the atoms, whereas the broad band at lower frequencies corresponds to (mostly) delocalized inter-tetrahedral motion [53,54].) For the case of the melt, however, the two curves differ significantly from each other. Although the general shape of  $\hat{K}(\omega)$  and  $g(\omega/2)$  are similar, the former quantity has a much smaller intensity at the two peaks at high frequencies but a

higher one in the broad band. Note that this “excess” in low frequency modes has nothing to do with the fact that  $K(t)$  shows at long times a  $\alpha$ -relaxation, whereas  $J(2t)$  does not, since at  $T = 3000\text{K}$  the typical frequencies of the  $\alpha$ -relaxation are smaller than  $1\text{THz}$ , and their contribution to the spectra can only be seen as the narrow peak at  $\omega = 0$  (see Fig. 2) [55]. Thus from this figure we can conclude that at low temperatures the harmonic approximation is very good whereas at intermediate temperatures significant deviations are observed.

Since  $c(z)$  is related to the Laplace transform of  $K(t)$ , see Eq. (24), one has to calculate this transform with high accuracy. From Fig. 1b we see however, that at low temperatures  $K(t)$  extends over many decades in time which makes the calculation of this transform a non-trivial matter. From this figure one also recognizes that, despite the large number of samples we used, the curves have still a significant amount of noise, most noticeable at long times and the lowest temperatures, since for these we used fewer samples. Since within the accuracy of the data the shape of the curves does, *in the late  $\alpha$ -relaxation regime*, not depend on temperature, we substituted for  $T \leq 4700\text{K}$  that part of the curve which was below 0.02 by the corresponding part of the curve for  $T = 6100\text{K}$ , after having it shifted to such large times that the resulting curve was smooth at 0.02. Subsequently the so obtained curves were smoothed and the Laplace transform calculated making use of the formula by Filon [56].

In Fig. 3 we show the real and imaginary part of  $c(z)$  for all temperatures investigated. (In the following we will assume  $z = \omega + i\epsilon$ , with  $\epsilon \rightarrow 0$ .) To discuss the frequency dependence of these curves let us focus for the moment on  $c'(\omega)$  for  $T = 2750\text{K}$ , the lowest temperature at which we could equilibrate our system. At very high frequencies  $c'(\omega)$  becomes independent of  $\omega$  and has a value of 1.5, which is the specific heat of an ideal gas. This result is reasonable since these high frequencies correspond to times at which the dynamics of each particle is not affected by the other ones, i.e., they move just ballistically. Upon lowering the frequency the specific heat rises rapidly since we are now in the frequency regime in which the dynamics of the system is mainly dominated by vibrations, see Fig. 2. Therefore at these frequencies the system can take up energy giving rise to the increase of  $c'(\omega)$ . Note that before this increase occurs,  $c'(\omega)$  shows a little dip around  $40\text{THz}$ , i.e., it falls below the ideal gas value. This dip can easily be understood by the harmonic picture proposed above, because the specific heat for a single harmonic oscillator shows a singularity at its resonance frequency. Since in our system we have many different oscillators that have typical frequencies between 1 and  $80\text{THz}$ , this singularity is smeared out and results in the dip and subsequent strong increase of  $c'(\omega)$ . The same mechanism is the reason for the little peak at around  $5\text{THz}$ .

If the frequency is decreased further,  $c'(\omega)$  stays constant until  $\omega^{-1}$  is on the order of the time scale of the  $\alpha$ -relaxation, i.e. the time scale of the structural relaxation. In this frequency range the system is again able to take up energy and hence  $c'(\omega)$  increases again. At even lower frequencies  $c'(\omega)$  becomes constant, i.e., it has reached the value of the *static* specific heat. This sequence of features in  $c'(\omega)$  can of course also be found in  $c''(\omega)$ , since the two functions are related by the Kramers-Kronig relation. In Fig. 3b we see that at high frequencies the imaginary part has a peak which corresponds to the vibrational excitations in the system. At much lower frequencies we find the  $\alpha$ -peak which corresponds to the structural relaxation process, i.e. the type of dynamics in which particles change their neighbors. For future reference we will introduce the terms “vibrational and configurational

part of the specific heat” by which we mean the height of the plateau in  $c'(\omega)$  at intermediate frequencies and the height of the step at low frequencies, respectively, and will denote them by  $c_{\text{conf}}$  and  $c_{\text{vib}}$ .

Let us now discuss the temperature dependence of  $c'(\omega)$  and  $c''(\omega)$ . From Fig. 3a we see that the specific heat at intermediate frequencies is essentially independent of  $T$ , since the vibrational motion of the ions is just a weak function of temperature. The main effect of an increase in temperature is that the height of the flat region at very small  $\omega$ , i.e. the static specific heat, increases, and that the crossover from this region to the plateau at intermediate frequencies moves to higher frequencies. At the highest temperature this crossover frequency has moved up to such high frequencies that no intermediate plateau is visible anymore, which means that in the system there is no longer a separation of time scales for the vibrational and relaxational processes. Furthermore we find that at the highest temperature the height of the plateau at small frequencies has decreased, i.e. that the value of the static specific heat has decreased. This effect is most likely related to the fact that silica shows a density anomaly, which for the present model occurs at around 4600K [5].

The temperature dependence just discussed is also found in the imaginary part of  $c(z)$  in that, with increasing temperature, the  $\alpha$ -peak moves continuously to higher frequencies until it merges with the microscopic peak. All this behavior is qualitatively similar to the one found for dynamic observables that measure the structural relaxation, such as the dynamic susceptibility [57,58]. Thus this gives evidence that the observable related to the structural relaxation and  $c(z)$  are closely connected to each other.

We also note that at low temperatures the form of the curves at low frequencies as well as their temperature dependence resembles very much the ones found in experiments [6–10,13]. The main difference is that in the simulation it is possible to measure  $c(z)$  even at such high frequencies that the effect of the microscopic vibrations becomes visible. Thus it is possible to follow continuously the evolution of  $c(z)$  from the microscopic regime to the mesoscopic one, i.e. to investigate the whole frequency dependence of  $c(z)$  from the liquid state to the viscous state. In contrast to this, experiments can probe only the frequency range below  $10^4\text{Hz}$  and therefore only the  $\alpha$ -regime is observable. However, since experimentally it is much simpler to equilibrate the material also at temperatures close to the glass transition temperature,  $c(z)$  can be measured at significantly lower temperatures than in a simulation.

Finally we mention that we have included in Fig. 3 also the data for  $T = 300\text{K}$ , i.e. a temperature at which the system is deep in the glass state. We see that this curve follows the pattern of the equilibrium curves very well in that it shows also the “harmonic resonance” at high frequencies and then a plateau at lower frequencies. No second plateau is seen in  $c'(\omega)$  (or an  $\alpha$ -peak in  $c''(\omega)$ ) at very small frequencies since at this temperature these features would occur at such low  $\omega$  that they are not visible within the time span of the simulation (or even an experiment).

Since the part of the specific heat that is related to the structural relaxation is the  $\alpha$ -relaxation peak at low frequencies, we will study this peak now a bit in more detail. In Fig. 4 we show an enlargement of this peak for intermediate and low temperatures. We clearly see that with decreasing temperature the area under the peak becomes smaller, which means that the configurational part of the specific heat decreases. This temperature dependence might be somewhat unexpected since for other dynamic susceptibilities, such as the one connected to the intermediate scattering function, one finds that the so-called time

temperature superposition principle is valid, i.e. a decrease in temperature just gives rise to a horizontal shift of the  $\alpha$ -peak [42,58]. However, since the area under the  $\alpha$ -peak is related via the Kramers-Kronig relation to the height of the step at low frequency in  $c'(\omega)$ , i.e. the configurational part of the specific heat, it is not surprising that this area depends on temperature, and below we will show that this is indeed the case. This tendency can also be easily understood from Eq. (24): For this we assume that in the  $\alpha$ -relaxation regime at low temperatures the function  $K(t)$  can be written as  $K(t, T) = f(T)\tilde{K}(t/\tau(T))$ , where  $f(T)$  is the height of the plateau and  $\tau(T)$  is the typical relaxation time. That this assumption is reasonable can be inferred from Fig. 1b. It is now simple to show that  $c''(\omega)$  can be approximated by  $c''(\omega) \approx \tilde{c}''(\omega\tau(T))f(T)/(1 - K(t=0))^2 = \tilde{c}''(\omega\tau(T))f(T)4(c_v^{eq})^2/9k_B^2$ , with a master function  $\tilde{c}''$ . (Here we also made use of Eq. (22)). Since the function  $\tilde{c}''$  is assumed to be independent of temperature, we see that the whole  $T$ -dependence of  $c''(\omega)$  is given by a shift in frequency proportional to  $\tau(T)$  and a vertical rescaling by  $f(T)(c_v^{eq})^2$ . Thus we conclude that the configurational part of the specific heat is proportional to  $f(T)(c_v^{eq})^2$ . For the present system both,  $f(T)$  and  $c_v^{eq}$ , decrease with decreasing temperature, and thus it is clear that the same is true for  $c_{\text{conf}}$ . However, in certain materials, such as fragile glass-formers, it is sometimes observed that the specific heat *increases* with decreasing temperature. Thus in these cases the temperature dependence of  $c_{\text{conf}}$  does not have to decrease monotonically, but it might, e.g., exhibit a local maximum.

Although the height of the  $\alpha$ -peak changes, its shape seems to be independent of temperature. To demonstrate this we plot in the inset of Fig. 4  $c''(\omega)/c''(\omega_{\text{max}})$  versus  $\omega/\omega_{\text{max}}$ , where  $\omega_{\text{max}}(T)$  is the location of the  $\alpha$ -peak. Since the curves for the different temperatures fall on top of each other, to within the accuracy of the data, we conclude that the shape does indeed not change with temperature. Also included in the figure is the Fourier transform of a Kohlrausch-Williams-Watts-law with a stretching exponent 0.9. We see that this functional form fits the master curve quite well, at least if one does not go to too high frequencies. At these higher frequencies the scaling breaks down due to the presence of the microscopic peak. We also mention that the (relatively large) value of the stretching parameter is reasonable, since in strong glass formers the stretching in the structural relaxation is usually weak, and indeed we have found that also for the present model the structural relaxation shows only a weak stretching [42].

Further evidence that the structural relaxation and the frequency dependent specific heat are closely connected to each other can be obtained by comparing the typical time scales for these functions. For this we have calculated the (incoherent) intermediate scattering function  $F_s(q, t)$  [48] for a wave-vector  $q = 1.7\text{\AA}^{-1}$ , which corresponds to the location of the first peak in the static structure factor [45]. We have defined the  $\alpha$ -relaxation time  $\tau_F^\alpha$ ,  $\alpha \in \{\text{Si}, \text{O}\}$ , by the time it takes this correlation function to decay to  $1/e$  of its initial value. To characterize the time scale for the specific heat we have determined from  $c''(\omega)$  the position of the maximum of the  $\alpha$ -peak and defined the relaxation time  $\tau_c$  as  $1/\omega_{\text{max}}$ . In Fig. 5 we show the temperature dependence of these relaxation times in an Arrhenius plot. From that graph we see that the relaxation times  $\tau_c$  and  $\tau_F^\alpha$  track each other very well in that at low temperatures both of them show an Arrhenius law with a very similar activation energy (numbers are given in the figure). With increasing temperature, deviations from this law are seen, the origin of which have been discussed elsewhere [45], but also these deviations are the same for both quantities. That the structural relaxation and the specific

heat do indeed track each other is demonstrated in the inset, where we plot the ratios  $\tau_F^\alpha/\tau_c$  as a function of inverse temperature. Since we see that these ratios are independent of temperature to within the accuracy of the data, we can conclude that the temperature dependence of the three quantities is indeed the same.

In the discussion of Fig. 3a we have mentioned that the increase in  $c'(\omega)$  at high frequencies is due to the vibrational degrees of freedom, whereas the step at lower frequencies is due to the relaxation of the configurational degrees of freedom. By measuring the heights of these two steps it thus becomes possible to determine the contribution of the vibrational and configurational degrees of freedom to the static specific heat and to investigate how these quantities depend on temperature [59]. The results obtained are shown in Fig. 6, where we plot  $c_v^{eq}$ , the value of  $c'(\omega)$  at very low frequencies which is hence the static specific heat,  $c_{\text{conf}}$ , the height of the step in  $c'(\omega)$  at low frequencies, and  $c_{\text{vib}}$ , the value of  $c'(\omega)$  at intermediate frequencies. Several observations can be made: Firstly,  $c_{\text{vib}}$  shows a very regular temperature dependence which can be approximated well by a linear function of temperature, at least in the temperature range investigated. An extrapolation of this temperature dependence to lower temperatures shows that  $c_{\text{vib}}$  attains the harmonic value of  $3k_B$  only at low temperatures ( $\approx 1000\text{K}$ ), i.e. at temperatures that are well below the (experimental) glass transition temperature, which is at  $1450\text{K}$  [62], a value that seems to be reproduced reasonably well by the present model [45]. Hence we find that  $c_{\text{vib}}$  is affected by anharmonic effects even at relatively low temperatures. We also mention that the vibrational part  $c_{\text{vib}}$  in the temperature range  $2750\text{K} \leq T \leq 3500\text{K}$  seems to be in nice agreement with a *linear* extrapolation of the experimental specific heat of the glass below  $T_g = 1450\text{K}$  to higher temperatures, i.e. if one leaves out the increase of the specific heat due to the glass transition.

The temperature dependence of  $c_{\text{conf}}$  is much more pronounced in than the one of  $c_{\text{vib}}$ , in that it shows around  $4000\text{K}$  a crossover from a relatively weak temperature dependence at high  $T$  to a stronger one at low  $T$ . Furthermore we see that  $c_{\text{conf}}$  is significantly smaller than  $c_{\text{vib}}$ , which is in agreement with the experimental result that strong glass formers show only a small drop in the specific heat when the temperature is lowered below the glass transition temperature, i.e. when the relaxational degrees of freedom are frozen [63]. We also note that for a strong glass former one expects that the Kauzmann temperature  $T_K$  is very small [64]. From the figure it seems however, that a naive extrapolation of  $c_{\text{conf}}$  to lower temperatures leads to a intercept with the temperature axis around  $T_{\text{conf}} \approx 2000\text{K}$ . Since the inequality  $T_{\text{conf}} \leq T_K$  must hold, this type of extrapolation thus leads to an estimate of  $T_K \geq 2000\text{K}$ . This high estimate of  $T_K$  is corroborated by recent results of the same model in which  $T_K$  was estimated by the direct calculation of the entropy and a subsequent extrapolation to lower temperatures [65].

These results for  $T_K$  depend of course crucially on the way  $c_{\text{conf}}$  is extrapolated to lower temperatures. From Fig. 6 it is clear that it is also possible to make this extrapolation in such a way that, e.g., at  $T = 1450\text{K}$  its value is around  $0.5k_B/\text{particle}$ , i.e. equal to the height of the step in the experimental curve at  $T_g$  (see experimental curves in figure) [66]. If the extrapolation is done in this way, the estimate of  $T_{\text{conf}}$  is moved to much lower temperatures. Thus it will be very interesting to attempt to do simulations at even lower temperatures in order to minimize the effects of this extrapolation. For this it will of course be necessary to equilibrate the system at even lower temperatures, which is computationally difficult. One

promising way to achieve this is the so-called method of “parallel tempering”, and work in this direction is presently done [67–69].

Also included in the figure is the specific heat of the system as calculated from the harmonic approximation [43] (dashed line). This was done by determining the eigenvalues of the dynamic matrix, and hence the density of states  $g(\omega)$ , and using the expression

$$c_v = \frac{h^2}{k_B T^2} \int_0^\infty \frac{\omega^2 g(\omega) \exp(h\omega/k_B T)}{(\exp(h\omega/k_B T) - 1)^2} d\omega. \quad (28)$$

More details on this calculation can be found in Ref. [43] where it has been shown that this theoretical curve agrees very well with experimental data below the glass transition temperature  $T_g$  (see the experimental data of Sosman [60] and Richet *et al.* [61], and the theoretical curve of Horbach *et al.* [43] in the figure). From the graph we see that an extrapolation of  $c_v^{eq}$  to lower temperatures extrapolates nicely to the experimental data and that an extrapolation of  $c_{vib}$  to lower temperatures can be joined smoothly to the curve from the harmonic approximation, thus showing that the two types of calculations are consistent with each other.

The expressions derived in Sec. II were valid for all wave-vectors  $q$  and only at the end, i.e. in Eq. (19), we restricted ourselves to  $q = 0$  in order to obtain the equation relating the frequency dependent specific heat to the temperature fluctuations. After having investigated so far the temperature dependence of  $c(z)$ , we now turn our attention to  $\Phi_{TT}(q, t)$ , the autocorrelation function of  $\delta T_q(t)$ , which measures the fluctuations in temperature at finite wave-vectors. From the definition of  $\Phi_{TT}(q, t)$  it is clear that this function should scale like  $T^2$ . That this is indeed the case is shown in Fig. 7, where we show  $\Phi_{TT}(q, t)/T^2$  for various wave-vectors and temperatures. Since for each wave-vector the curves for the different temperatures fall on top of each other we recognize immediately that the  $T^{-2}$  dependence is correct. Note that this weak temperature dependence for  $q > 0$  is in strong contrast to the one found for  $q = 0$  (see Fig. 1b). It reflects the fact that the thermal conductivity  $\lambda$  is only a weak function of temperature, see Eq. (26).

From the plot we also see that the typical time scale over which the correlation functions decay, increases with decreasing wave-vector, in qualitative agreement with Eq. (26) which predicts a  $q^{-2}$  dependence. To determine the  $q$ -dependence of this decay we define a decay time  $\tau(q)$  as the time it takes the correlation function to decay to 0.1 of their initial value. The wave-vector dependence of  $\tau(q)$  is shown in Fig. 8 where we plot  $q^2 \tau(q)$  versus  $q^2$ . (Since within the accuracy of our data the temperature dependence of  $\Phi_{TT}(q, t)$  is independent of  $T$  we show only one set of data points.). From this figure we recognize that for small wave-vectors the relaxation time scales indeed like  $q^{-2} + const$ , as expected from hydrodynamics (straight line), that however, this linear dependence breaks down for large wave-vectors. Furthermore we see that the slope of this straight line is positive, which means that the second term in Eq. (26) is larger than zero. From this equation it follows that the intercept of the straight line with the abscissa is given by  $n c_p^{eq} / \lambda$ , where  $n$  is the particle density and  $\lambda$  is the thermal conductivity. We read off an intercept  $0.0180 \text{ ps}/\text{\AA}^2$  and with the specific heat of  $4k_B$  per particle, see Fig. 3a, we obtain  $\lambda = 2.4 \text{ W/Km}$ . This value is in good agreement to the one determined by a completely different method in the simulation by Jund and Jullien who found  $\lambda \approx 1.3 \text{ W/Km}$  around  $1000 \text{ K}$  [44]. The experimental values for this quantity range between 2 and  $3 \text{ W/Km}$  at high temperatures if  $T \geq 1000 \text{ K}$  [49],



i.e. our value is in agreement also with the experimental data. (Note that in experiments it is found that the  $\lambda$  is a strong function of temperature for temperatures below  $\approx 1000\text{K}$ . For higher temperatures it seems, however, to level off and thus it can be extrapolated reasonably safely to temperatures in the melt. Since this temperature dependence of  $\lambda$  is due to anharmonicities one can conclude that these become effectively independent of  $T$  in the temperature range of the supercooled melt.)

## V. SUMMARY AND DISCUSSION

The goal of this paper is to show how the frequency dependent specific heat,  $c_v(z)$ , is related to the dynamics of the particles on the microscopic level. For this we use the Mori-Zwanzig projection operator formalism to derive an exact expression for  $c_v(z)$  (Eq. (17)). This expression allows us to identify the physical mechanism which causes the frequency dependence of  $c_v(z)$ , namely the relaxation of the potential energy during the structural relaxation. Using an exact transformation formula by Lebowitz *et al.*, we obtain an equation which relates  $c_v(z)$  to the Laplace transform of  $K(t)$ , the autocorrelation function of temperature fluctuations (Eq. (24)) in the microcanonical ensemble, and which thus can be used to determine  $c_v(z)$  from a computer simulation. This relation has been derived previously by Nielsen [24] on the basis of thermodynamic arguments. In contrast to that approach we are, however, also able to generalize the correlator  $K(t)$  to finite wave-vectors and to relate the time dependence of these quantities to the thermal conductivity of the system, Eq. (26).

By using molecular dynamics computer simulations of a simple but quite realistic model for silica, we have determined the time and temperature dependence of  $K(t)$ . We see that at low temperatures this correlator shows a two-step decay, similar to the one that is found in the time correlation functions for structural quantities, such as the intermediate scattering function. In contrast to these correlators the height of the plateau at intermediate times *decreases* with decreasing temperature, a trend that can be understood by realizing that at very low temperatures  $K(t)$  is directly related to the autocorrelation function of the velocity.

From the time dependence of  $K(t)$  we have calculated the frequency dependent specific heat. In contrast to previous numerical investigations the accuracy of our data is high enough to analyze in detail the frequency dependence of the real and imaginary part of  $c(z)$ . We find that at very high frequencies the value of  $c'(\omega)$  is the one of an ideal gas and that with decreasing frequency it shows a rapid increase which is due to the vibrational excitations of the system. At low temperatures we see that  $c'(\omega)$  shows a second increase at frequencies which correspond to the time scales of the structural relaxation. This frequency dependence is also reflected in  $c''(\omega)$  where the first and second increase are reflected by the microscopic and  $\alpha$ -peak, respectively. Thus we find that the frequency dependence of  $c(z)$  is qualitatively very similar to the one found in the dynamical susceptibility for structural quantities, which shows how intimately connected these quantities are. Further evidence for this can be obtained from the observation that the location of the  $\alpha$ -peak in  $c''(\omega)$  shows the same temperature dependence as the structural relaxation, in agreement with experimental findings [10,12,13].

From the height of the two mentioned steps in  $c'(\omega)$ , we are able to determine the vibrational and the configurational part of the specific heat. We find that the former is

significantly higher than the latter, which is in agreement with the experimental observation that in strong liquids the drop in the specific heat at the glass transition is relatively small.

Finally we have calculated the time dependence of the autocorrelation functions of temperature fluctuations at finite wave-vectors. In agreement with our theoretical prediction, these functions decay much faster than the one for  $q = 0$ , i.e.  $K(t)$ , and depend only very weakly on temperature. From the  $q$ -dependence of the relaxation time of this correlator we calculate the thermal conductivity  $\lambda$  and find good agreement of our value with the one in experiments and a computer simulation in which  $\lambda$  was determined by a different method.

We also point out that, since our simulations have been done at constant volume, it is clear that the frequency dependence of  $c(z)$  and the strong temperature dependence of  $\omega_{max}$ , the location of the  $\alpha$ -peak in  $c''(\omega)$ , is *not* the result of the frequency and temperature dependence of the macroscopic density. Some time ago Zwanzig proposed (essentially) the following mechanism for the  $T$ -dependence of  $\omega_{max}$  [20]: A change in temperature will in general give rise to a change in density (since most real experiments are done at constant pressure and not density). Due to the high value of the bulk viscosity, this volume relaxation will be slow and occur on the time scale of the  $\alpha$ -relaxation, and hence  $c_p$  will be frequency dependent. Since in turn the frequency dependence of the viscosity is due to the slow relaxation of the structure on the microscopic scale, Zwanzig thus argued that the reason for the  $T$ -dependence of  $\omega_{max}$  is just an *indirect* effect of the slow microscopic dynamics. Since in a system with constant volume this mechanism is not present and our simulations demonstrate that  $\omega_{max}$  does show a strong  $T$ -dependence, we conclude that the reason for this dependence must be a different one.

Finally we also mention that from the shape of the  $\alpha$ -peak in  $c''(\omega)$  it is also possible to calculate the time dependence of the enthalpy in a cooling and heating experiment. For this we made simulations in which the sample was first cooled with a finite cooling rate through the glass transition temperature and subsequently reheated above  $T_g$ . Using the *equilibrium* data for  $c(z)$  we were able to reproduce accurately the time and temperature dependence of the enthalpy [15,16], which shows that if one knows the *equilibrium* quantity  $c(z)$ , one is also able to predict the system in an out-of-equilibrium situation.

Acknowledgments: We thank U. Fotheringham and F. Sciortino for useful discussions. This work was supported by Schott Glas and the DFG under SFB 262. Part of this work was done at the HLRZ in Jülich.

## APPENDIX A: RELATION BETWEEN THE DENSITY OF STATES AND THE AUTOCORRELATION FUNCTION OF THE KINETIC ENERGY FOR A HARMONIC SYSTEM

For a purely harmonic system with the Hamiltonian

$$H = \frac{\mathbf{p}^2}{2m} + \frac{m\Omega^2 \mathbf{r}^2}{2} \quad (\text{A1})$$

momenta and space coordinates are Gaussian variables. This simplifies considerably the evaluation of the normalized autocorrelation function of the kinetic energy  $K(t)$ . For a set of Gaussian variables with zero mean the four point correlation function  $\langle ABCD \rangle$  can be expressed by the two point correlation functions:

$$\langle ABCD \rangle = \langle AB \rangle \langle CD \rangle + \langle AC \rangle \langle BD \rangle + \langle AD \rangle \langle BC \rangle. \quad (\text{A2})$$

Using this relation, the autocorrelation function  $\langle p_\mu^2(t)p_\nu^2 \rangle$  can be written as

$$\langle p_\mu^2(t)p_\nu^2 \rangle = 2\langle p_\mu(t)p_\nu \rangle^2 + \langle p_\mu^2 \rangle \langle p_\nu^2 \rangle \quad . \quad (\text{A3})$$

Since  $\langle p_\mu(t)p_\nu \rangle = \delta_{\mu\nu} \langle p_\mu^2 \rangle \cos \Omega t$ , the autocorrelation function  $\Phi_{TT}(t)$  is given by

$$\Phi_{TT}(t) = \frac{1}{9m^2k_B^2} (\langle \mathbf{p}^2(t)\mathbf{p}^2 \rangle - \langle \mathbf{p}^2 \rangle^2) \quad (\text{A4})$$

$$= \frac{2}{9m^2k_B^2} \sum_{\mu} \langle p_\mu(t)p_\mu \rangle^2 \quad (\text{A5})$$

$$= \frac{T^2}{3} (\cos(2\Omega t) + 1) \quad . \quad (\text{A6})$$

All averages are in the canonical ensemble and we used that  $\langle p_\mu^2 \rangle = k_B T$ . From Eq. (21) we know, by using the value of the specific heat of a harmonic oscillator in three dimensions  $c_v^{eq} = 3k_B$ , that  $\Phi_{TT}^{(mc)}(t) = \Phi_{TT}(t) - T^2/3$ . By defining the velocity autocorrelation function  $J(t) = m \langle \mathbf{v}(t)\mathbf{v} \rangle$  and noting, that for a harmonic oscillator  $(\vec{v}(t)|\vec{v}) = 3k_B T/m \cos(\Omega t)$  we obtain the result

$$K(t) = \frac{J(2t)}{6k_B T} \quad . \quad (\text{A7})$$

Taking the Fourier transform of (A7) and using, that the density of states  $g(\omega) = 2J(\omega)/3k_B T$  [52], we arrive at the result

$$\hat{K}(\omega) = \frac{g(\omega/2)}{8} \quad . \quad (\text{A8})$$

## REFERENCES

- [1] J. Zarzycki (Ed.), Vol. 9 of *Materials Science and Technology* (VHC, Weinheim, 1991); A. Feltz, *Amorphous Inorganic Materials and Glasses* (VCH, Weinheim, 1993); P. G. Debenedetti, *Metastable Liquids* (Princeton University Press, Princeton, 1997).
- [2] W. Götze, p. 287 in *Liquids, Freezing and the Glass Transition* Eds.: J.-P. Hansen, D. Levesque, and J. Zinn-Justin, Les Houches. Session LI, 1989 (North-Holland, Amsterdam, 1991);  
W. Götze, J. Phys.: Condens. Matter **10A**, 1 (1999).
- [3] Note that this definition of  $T_g$  is not the same as the one often used and which is defined by requiring that at  $T_g$  the viscosity of the system is  $10^{13}$  Poise.
- [4] R. Brüning and K. Samwer, Phys. Rev. B **46**, 11318 (1992).
- [5] K. Vollmayr, W. Kob, and K. Binder, Phys. Rev. B **54**, 15808 (1996).
- [6] N. O. Birge and S. R. Nagel, Phys. Rev. Lett. **54**, 2674 (1985).
- [7] N. O. Birge, Phys. Rev. B. **34**, 1631 (1986).
- [8] P. K. Dixon and S. R. Nagel, Phys. Rev. Lett. **61**, 341 (1988).
- [9] P. K. Dixon, Phys. Rev. B **42**, 8179 (1990).
- [10] N. Menon, J. Chem. Phys. **105**, 5246 (1996).
- [11] T. Christensen, J. de Phys. (France) Coll. C8, **46**, 635 (1985).
- [12] H. Leyser, A. Schulte, W. Doster, and W. Petry, Phys. Rev. E **51**, 5899 (1995).
- [13] Y. H. Jeong and I. K Moon, Phys. Rev. B **52**, 6381 (1995).
- [14] M. Beiner, J. Korus, H. Lockwenz, K. Schröter, and E. Donth, Macromol. **29**, 5183 (1996).
- [15] P. Scheidler, Diploma Thesis (Universität Mainz, 1999).
- [16] P. Scheidler, W. Kob, and K. Binder, to be published.
- [17] S. L. Simon and G. B. McKenna, J. Chem. Phys. **107**, 8678 (1997).
- [18] D. W. Oxtoby, J. Chem. Phys. **85**, 1549 (1986).
- [19] J. Jäckle, Z. Phys. B **64**, 41 (1986).
- [20] R. Zwanzig, J. Chem. Phys. **88**, 5831 (1988).
- [21] W. Götze and A. Latz, J. Phys.: Condens. Matter **1**, 4169 (1989).
- [22] J. K. Nielsen and J. C. Dyre, Phys. Rev. B **54**, 15754 (1996).
- [23] J. Jäckle, Physica A **162**, 377 (1990).
- [24] J. K. Nielsen, Phys. Rev. E **60**, 471 (1999).
- [25] G. S. Grest and S. R. Nagel, J. Phys. Chem. **91**, 4916 (1987).
- [26] S. R. Nagel, private communications.
- [27] D. Forster, *Hydrodynamic Fluctuations, Broken Symmetry, and Correlation Fluctuations* (Benjamin Cummings, London, 1983).
- [28] R. A. Ferrell and J. K. Bhattacharjee, Phys. Rev. A **31**, 1788 (1985) and references therein.
- [29] In Eq. (15) we made use of the relation  $Q_\rho E_q^P \equiv Q_\rho Q E_q^P \equiv Q E_\rho^P$ .
- [30] P. Schofield, Proc. Phys. Soc. **88**, 149 (1966).
- [31] A. Latz, PhD thesis (TU München, 1991).
- [32] Note that in equilibrium the specific heat at constant volume and constant pressure are related by  $c_p - c_v = TV\alpha^2/\kappa_T n$ , where  $\alpha$  is the thermal expansion coefficient and  $\kappa_T$  is the isothermal compressibility. For the frequency dependent case this relation is

- generalized to  $c_p(z) - c_v(z) = T\alpha^2(z)K_B(z)/N$ , where  $\alpha(z) = V^{-1}\partial V(z)/\partial T(z)$  is the frequency dependent thermal expansion coefficient [21,31].
- [33] T. Franosch, M. Fuchs, and A. Latz, preprint cond-mat/0006214 (2000).
  - [34] J. L. Lebowitz, J. K. Percus, and L. Verlet, Phys. Rev. **153**, 250 (1967).
  - [35] Note that a simple calculation shows that the RHS of this equation does *not* decay to zero for long times, whereas  $\Phi_{TT}^{(mc)}(t)$  does.
  - [36] B. W. H. van Beest, G. J. Kramer, and R. A. van Santen, Phys. Rev. Lett. **64**, 1955 (1990).
  - [37] K. Vollmayr and W. Kob, Ber. Bunsenges. Phys. Chemie **100**, 1399 (1996).
  - [38] T. Koslowski, W. Kob, and K. Vollmayr, Phys. Rev. B **56**, 9469 (1997).
  - [39] S. N. Taraskin and S. R. Elliott, Europhys. Lett. **39**, 37 (1997).
  - [40] S. N. Taraskin and S. R. Elliott, Phys. Rev. B **56**, 8605 (1997).
  - [41] J. Horbach, W. Kob, and K. Binder, J. Non-Cryst. Solids **235–237**, 320 (1998).
  - [42] J. Horbach, W. Kob, and K. Binder, Phil. Mag. B **77**, 297 (1998).
  - [43] J. Horbach, W. Kob, and K. Binder, J. Phys. Chem. B **103**, 4104 (1999).
  - [44] P. Jund and R. Jullien, Phys. Rev. B **59**, 13707 (1999).
  - [45] J. Horbach and W. Kob, Phys. Rev. B **60**, 3169 (1999).
  - [46] M. Benoit, S. Ispas, P. Jund, and R. Jullien, Eur. Phys. J. B **13**, 631 (2000).
  - [47] J. Horbach, W. Kob, and K. Binder, preprint cond-mat/9910445.
  - [48] J.-P. Hansen and I. R. McDonald, *Theory of Simple Liquids* (Academic, London, 1986).
  - [49] O. V. Mazurin, M. V. Streltsina, and T. P. Shvaiko-Shvaikovskaya, *Handbook of Glass Data, Part A: Silica Glass and Binary Silicate Glasses* (Elsevier, Amsterdam, 1983).
  - [50] J. Horbach, W. Kob, K. Binder, and C. A. Angell, Phys. Rev. E. **54**, R5897 (1996).
  - [51] W. H. Press, B. P. Flannery, S. A. Teukolsky, and W. T. Vetterling, *Numerical Recipes* (Cambridge University Press, Cambridge, 1986).
  - [52] M. T. Dove, *Introduction to Lattice Dynamics* (Cambridge University Press, Cambridge, 1993).
  - [53] F. L. Galeener, Phys. Rev. B **19**, 4292 (1979).
  - [54] A. Pasquarello and R. Car, Phys. Rev. Lett. **80**, 5145 (1998).
  - [55] Note that the finite width of the peak at  $\omega = 0$  as shown in the figure is due to our finite resolution.
  - [56] M. Abramowitz and I. A. Stegun, *Handbook of Mathematical Functions* (Dover, New York, 1964).
  - [57] J. Horbach, PhD Thesis (Universität Mainz, 1998).
  - [58] J. Horbach and W. Kob, to be published.
  - [59] Note that at intermediate and high temperatures the  $\alpha$ -peak and the microscopic process are not separated well from each other. Thus in order to determine the height of the low-frequency step in  $c'(\omega)$  it is necessary to extrapolate this step to higher frequencies. This was done by means of the sum of two Kohlrausch-Williams-Watts laws, which at this point should be considered as mere fitting functions without physical significance. More details on this can be found in Ref. [15].
  - [60] R. B. Sosman, *The Properties of Silica* (Chemical Catalog Company, New York, 1927).
  - [61] P. Richet, Y. Bottinga, D. Denielou, J. P. Petitet, and C. Tegui, Geochim. Cosmochim. Acta **46**, 2639 (1982).
  - [62] R. Brückner, J. Non-Cryst. Solids **5**, 123 (1970).

- [63] C. A. Angell, P. H. Poole, and J. Shao, *Nuovo Cimento D* **16**, 993 (1994).
- [64] C. A. Angell, in *Relaxation in Complex Systems*, Eds.: K. L. Ngai and G. B. Wright (US Dept. Commerce, Springfield, 1985).
- [65] I. Saika-Voivod, (unpublished).
- [66] Note that the experimental values are for  $c_p$  whereas the theoretical ones are for  $c_v$ . However since for silica the thermal expansion coefficient  $\alpha$  is very small [49], the difference between  $c_p$  and  $c_v$  is also small, as can be seen from the relation  $c_p - c_v = T\alpha^2/\kappa_T n$ , where  $\kappa_T$  is the isothermal compressibility.
- [67] T. Stühn, Diploma Thesis (Universität Mainz, 2000).
- [68] R. Yamamoto and W. Kob, *Phys. Rev. E* **61**, 5473 (2000).
- [69] W. Kob, C. Brangian, T. Stühn, and R. Yamamoto, to appear in “Computer Simulation Studies in Condensed Matter Physics XIII”; Eds. D. P. Landau, S. P Lewis, and H. B. Schüttler (Springer, Berlin, 2000).

FIGURES

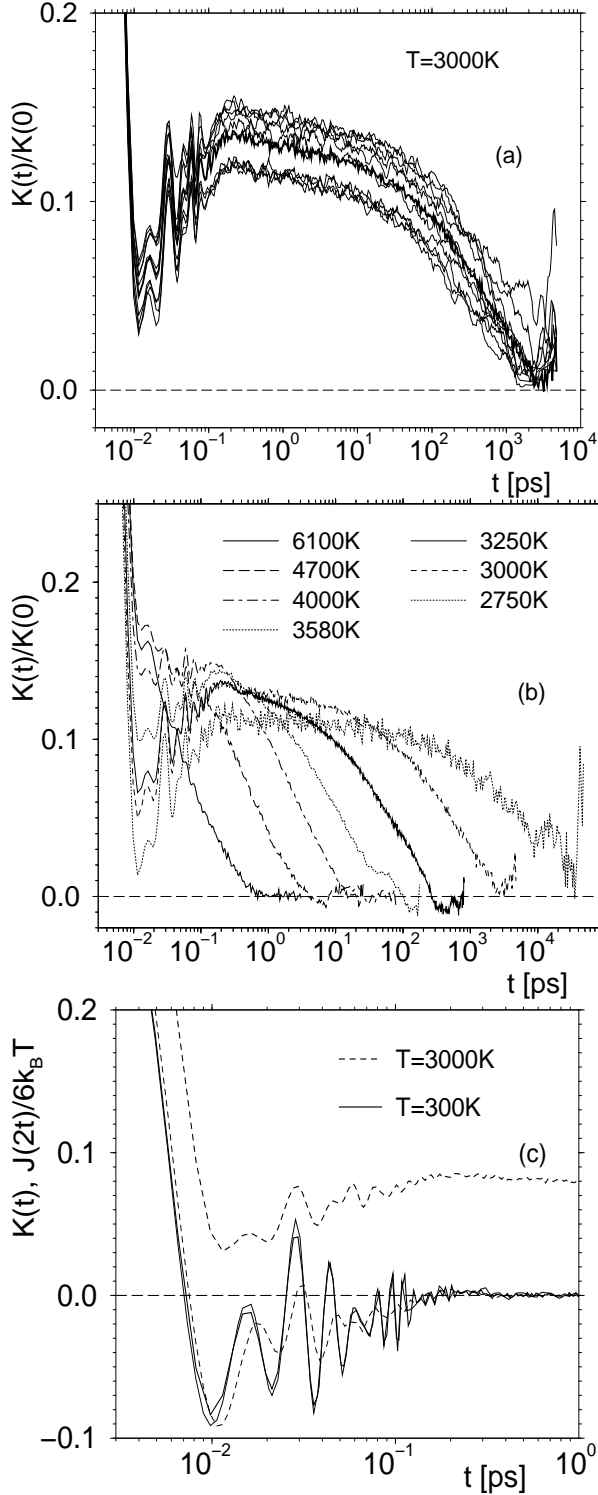


FIG. 1. Time dependence of the normalized kinetic energy autocorrelation function. a)  $T = 3000\text{K}$ ; each thin curve is the average over ten different samples; the average over these curves gives the bold curve. b)  $K(t)/K(0)$  for all temperatures investigated. c) Bold curves:  $K(t)$  for  $T = 3000\text{K}$  and  $T = 300\text{K}$ ; thin curves: velocity-autocorrelation function  $J(2t)/6k_B T$  (see Appendix A) at the same temperatures.

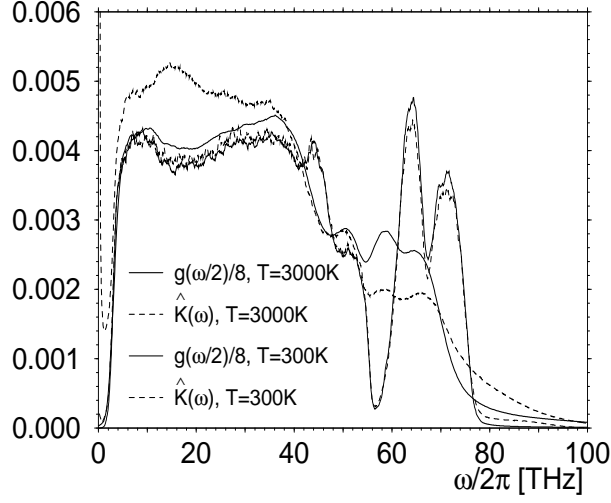


FIG. 2. Frequency dependence of  $\hat{K}(\omega)$  and  $g(\omega/2)/8$  (dashed and solid curves, respectively). Bold lines:  $T = 3000\text{K}$ , thin lines:  $T = 300\text{K}$ .

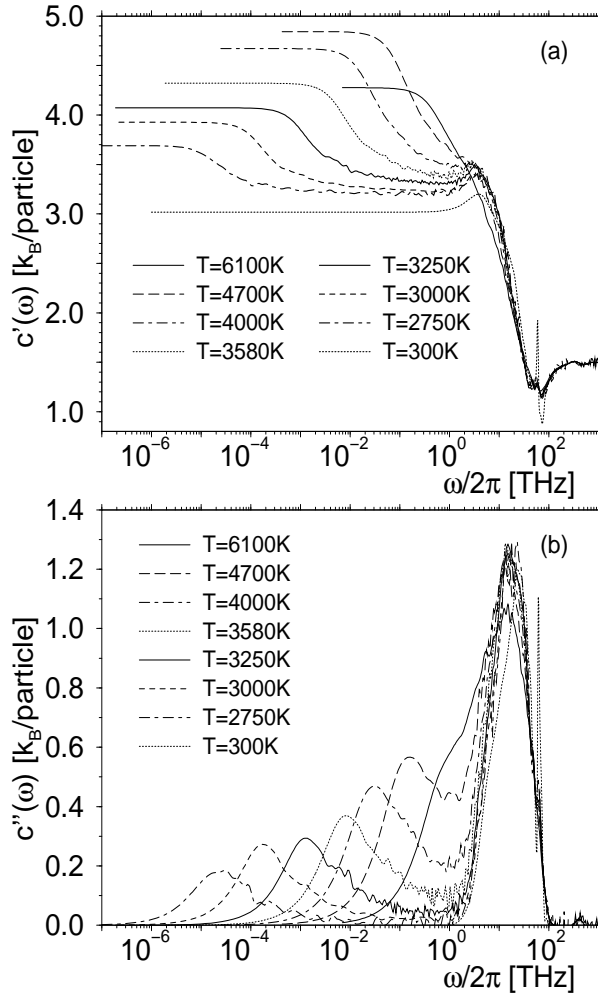


FIG. 3. Frequency dependence of the specific heat for all temperatures investigated. a) Real part. b) Imaginary part.



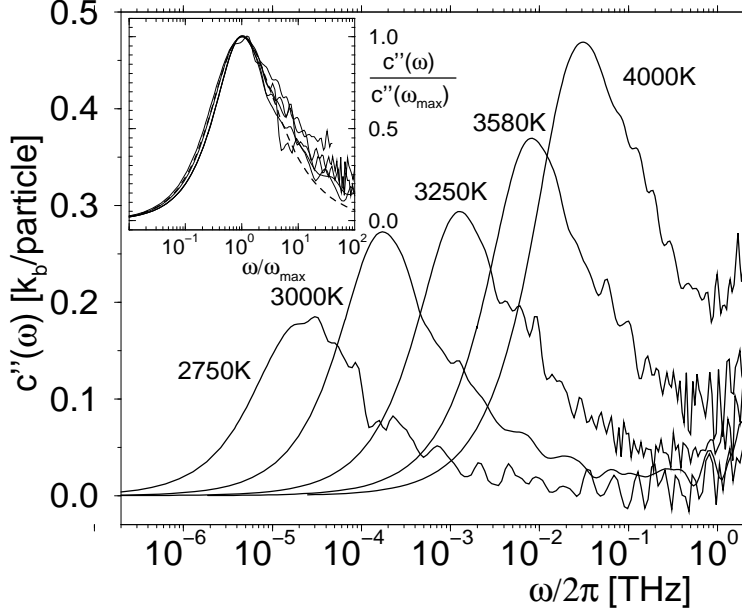


FIG. 4. Main figure: Frequency dependence of the  $\alpha$ -peak for intermediate and low temperatures. Inset: Same curves scaled by the height of their maximum versus  $\omega/\omega_{\max}$ , where  $\omega_{\max}$  is the location of the maximum. Dashed line: Kohlrausch-Williams-Watts function.

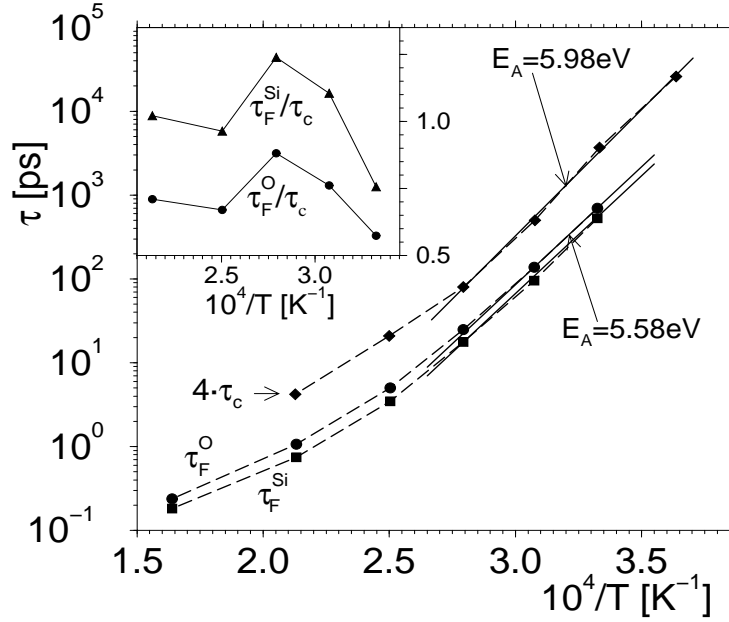


FIG. 5. Main figure: Temperature dependence of the  $\alpha$ -relaxation times as determined from the incoherent intermediate scattering function and the frequency dependent specific heat. The straight lines are fits with an Arrhenius law. Inset: ratio of these relaxation times.

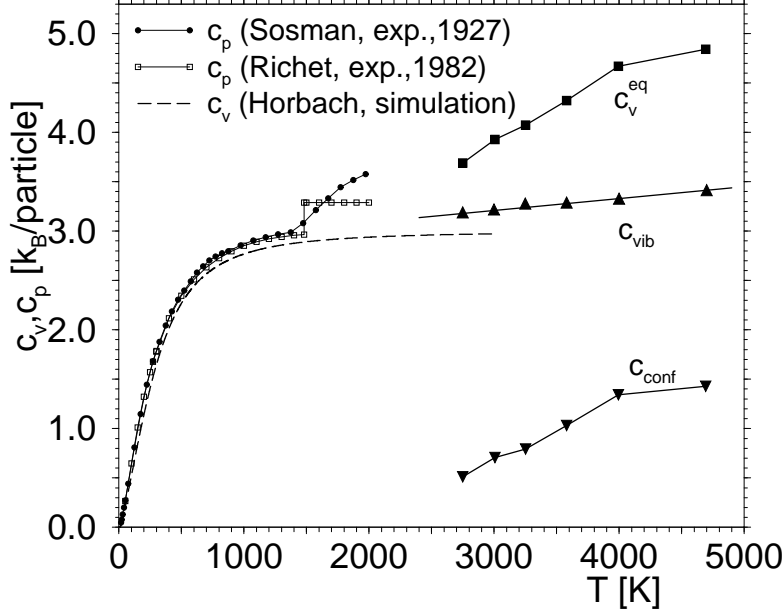


FIG. 6. Temperature dependence of  $c_{conf}$  and  $c_{vib}$ , the configurational and vibrational part of the specific heat, respectively, and of their sum  $c_v^{eq}$ . The dashed line is the specific heat as calculated from the harmonic approximation [43]. The curves with the small symbols are experimental data from Ref. [60,61].

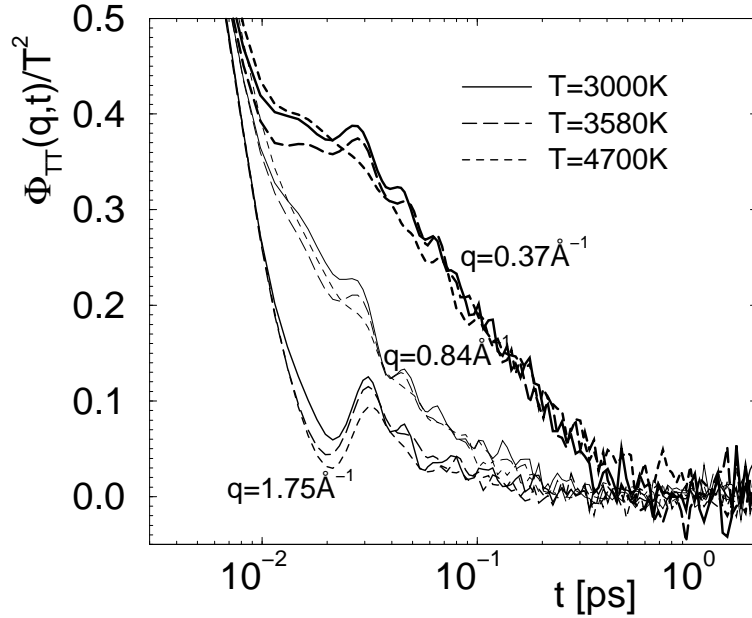


FIG. 7. Time dependence of the autocorrelation function of the generalized temperature fluctuations  $\delta T_q(t)$ . The different line styles correspond to different temperatures and the different thickness to different wave-vectors.

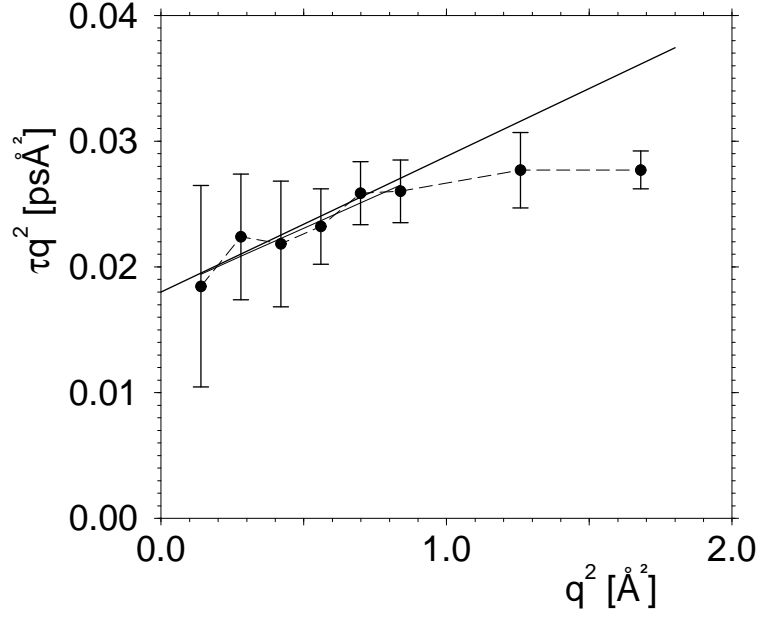


FIG. 8. Relaxation time for the autocorrelation function  $\Phi_{TT}(q, t)/T^2$  multiplied by  $q^2$  versus the square of the wave-vector. The straight line is a fit with the functional form given by Eq. (26). This line is given by  $q^2\tau = 0.0180\text{ps}\text{\AA}^{-2} + 0.0101q^2\text{ps}$ .